Macromolecules 1992, *25*, 6240–6247

Characterization of Diblock Copolymer Monolayers at the Liquid–Air Interface by Neutron Reflectivity and Surface Tension Measurements

Michael S. Kent,[*,†,‡] **Lay-Theng Lee,**[§] **Bernard Farnoux,**[§] **and Francis Rondelez**[‡]

Laboratoire de Physico-Chimie des Surfaces et Interfaces (associé au CNRS-URA 1379 et à l'Université Paris VI), Institut Curie, Section de Physique et Chimie, 11 rue Pierre et Marie Curie, 75005 Paris, France, and Laboratoire Léon Brillouin (CEA-CNRS), CEN-Saclay, 91191 Gif-sur-Yvette Cedex, France

Received March 5, 1992; Revised Manuscript Received July 6, 1992

ABSTRACT: We report simultaneous measurements of the concentration profile and the free energy of the submerged PS blocks of PDMS–PS diblock copolymers spread as monolayers at the air surface of ethyl benzoate as a function of surface concentration. A parabolic concentration profile is found to give the best fit to neutron reflectivity curves among the set of two-parameter models examined. The maximum extension h^*/R_g is comparable to previously reported values obtained from a variety of techniques for similar values of the reduced surface density σ^* and indicates some stretching perpendicular to the surface. As σ^* increases from 1.3 to 4.2, the energy per PS block (obtained from surface tension measurements) increases sharply while the dependence of h^* on σ^* is much weaker than the $^1/_3$ power law dependence predicted for the strongly stretched regime. Thus, the energy required to stretch the chains for this system appears to be much larger than predicted by current theories.

Introduction

Block copolymers tend to straddle interfaces and therefore have a great potential for altering interfacial properties. Important industrial uses include strengthening the interface between incompatible polymer blends, stabilizing colloidal dispersions, and use as polymeric analogues to the more common small-molecule surfactants. A useful unifying concept for the description of these systems as well as for grafted chain systems and highly branched polymers is that of a "tethered" chain, that is, a chain which is anchored at one end to a point or an interface.[1] A key variable for these systems is the degree of crowding of the tethered chains. For chains tethered to a plane surface, this can be expressed as $\sigma^* = \sigma/\sigma_{ol}$, where σ is the surface density (number of chains per unit area), $\sigma_{ol} = 1/\pi R_g^2$ is an estimate of the surface density for which the tethered chains just begin to overlap, and R_g is the root mean square (rms) radius of gyration of a free coil in solution. The equilibrium concentration profile, which will determine many important physical properties of the system, has been calculated in a good solvent by balancing the osmotic repulsion between polymer segments, which tends to make the chains stretch perpendicular to the surface in order to decrease the segmental concentration, with the elastic restoring force arising from the decrease in chain entropy. Assuming a steplike profile and uniform stretching of the chains, Alexander[2] was the first to predict $L \propto N\sigma^{1/3}$ where L is the height of the polymer brush and N is the number of monomers per chain. More elaborate self-consistent mean-field approaches including both analytical theories[3,4] and numerical solutions[5–8] support the same scaling law for intermediate σ but give a more precise description of the profile which contains a region of depleted monomer concentration near the surface (for chains which do not adsorb) followed by a parabolic decay from the maximum rather than a step function. Finally, the outer region of the profile decays smoothly to zero instead of the rather sharp cutoff of the parabolic profile. The profile becomes more steplike at very high σ, as the chains must eventually pack as rods.

Experimental approaches to the study of tethered chain systems have included the direct measurement of force versus distance profiles for two surfaces coated by selectively adsorbed block copolymers or end-grafted chains,[9–13] SANS and NMR from chains end-grafted onto silica particles,[14–18] neutron reflectivity from selectively adsorbed block copolymers at the solid–liquid interface,[19–21] and Monte Carlo (MC)[7,22] and molecular dynamics (MD)[23] simulations. In the direct force measurements involving layers of poly(2-vinylpyridine)–polystyrene (P2VP–PS) diblock copolymers in which the P2VP block adsorbed strongly to mica and the PS block extended out into the good solvent toluene,[9,10] the onset of a measurable force has been reported for distances of separation up to 10 times the radius of gyration of the PS block. Assuming a parabolic profile, this implies on rms average chain dimension perpendicular to the surface of roughly $2R_g$. A similar observation has been reported for adsorbed layers of poly(ethylene oxide)–polystyrene (PEO–PS) diblock copolymers, where the PEO block adsorbs selectively onto mica from toluene, and for layers of PS chains end-grafted onto the mica surface in toluene.[12,13] Other experiments involving layers of tethered chains have also indicated dimensions perpendicular to the interface greater than R_g.[15–17,18,20,21]

Several comparisons with the predicted scaling laws have been reported. In the studies involving the force-balance apparatus, the force-distance profiles were reported to scale with the variables N and σ in a manner consistent with the above theories,[11,12] although it has not been possible thus far to vary both N and σ independently. The same PEO–PS/toluene system previously studied in refs 12 and 13 by the force-balance technique has recently been reexamined by neutron reflectivity (where the PEO block selectively adsorbs onto a flat quartz surface).[21] In both experiments good agreement was reported with $L \propto N\sigma^{1/3}$ for a range of σ^* from 4 to 7. Strong support for $L \propto N\sigma^{1/3}$

---

[*] To whom all correspondence should be addressed.

[†] Permanent address: Division 1815, Sandia National Laboratories, Albuquerque, NM 87185.

[‡] Institut Curie.

[§] CEN-Saclay.

0024-9297/92/2225-6240$03.00/0

for $\sigma^* > 10$ has been reported by Auroy et al.,[15-17] who have recently synthesized a series of grafted chain systems (PDMS end-grafted onto silica particles) covering a large range of N and σ which were studied by SANS. The MC and MD simulations have also supported this scaling law, with the latter indicating a lower limit of $N\sigma^{1/3}$ ($\sim$15) below which this scaling no longer holds. Experimentally, the precise range of σ and N for which the scaling law holds has not been firmly established. For example, for the range of σ^* for which $L \propto N\sigma^{1/3}$ has been reported to hold in the work of Taunton et al.[12] and Field et al.[21] (roughly 4–7), virtually no variation of L with σ is observed in the work of Auroy et al.[17]

In reference to the concentration profile, there has not yet been a clear determination of its precise shape, although several groups have concluded that the profile must be smoother than a step function.[14,17,20,21] Cosgrove et al.[20] and Field et al.,[21] in particular, have reported that both exponential and step profiles were inadequate to describe their neutron reflectivity data from selectively adsorbed block copolymers at the solid–liquid interface (with σ^* ranging from 4 to 7), while the data were consistent with a parabolic function. In addition, previous SANS data of Cosgrove et al.[14] have suggested the presence of a depletion layer near the surface. The MC and MD simulations have also supported the parabolic profile with a depletion layer near the surface at intermediate σ, with the latter giving the regions in depth and the range of $N^{3/5}\,\sigma^{1/2}$ for which the profile may be considered consistent with the parabolic profile.

We have previously submitted a brief report[24] describing the first use of neutron reflectivity to study diblock copolymers spread as monolayers at the liquid–air interface. In this report we present a much more complete set of data on two diblock copolymers which vary mainly in the molecular weight of the anchoring block. The diblock copolymer is polydimethylsiloxane–polystyrene (PDMS–PS), which has been found to spread and form stable monolayers on the surface of ethyl benzoate (EB). EB is a good solvent for PS but a nonsolvent for PDMS. This is a tethered chain system, as the PS block is soluble in the solvent but is anchored to the surface by the PDMS block which remains on the surface. In addition to being a selective solvent for PS, the surface tension (γ) of EB lies between that of PS and PDMS ($\gamma_{EB} \cong 34$ dyne/cm, $\gamma_{PDMS} \cong 20$ dyne/cm, $\gamma_{PS} \cong 40$ dyne/cm).[25] Since $\gamma_{PDMS} < \gamma_{EB}$, there is a strong driving force for the PDMS block to remain at the surface. Moreover, the fact that $\gamma_{EB} < \gamma_{PS}$ ensures that the PS block does not adsorb at the surface. This is to be contrasted with the liquid–solid interface, where high surface energies and specific adsorption sites often lead to some adsorption.

This system offers a combination of features useful for testing theoretical predictions not possible with adsorbed or grafted systems at the liquid–solid interface. First, there is great potential for measuring the concentration profile in detail. Neutron reflectivity is proven to be a powerful technique for measuring polymer concentration profiles near interfaces.[19-21,26] This is particularly true at the air surface of a liquid, as the low surface roughness ($\sim$5 Å) in principle allows measurements to higher values of the momentum transfer q than for solid–liquid interfaces. In addition, problems associated with a monolayer of chemisorbed water which is believed to be present at a quartz or mica surface are avoided.[21] In the present system, hydrogenated PDMS is nearly contrast matched with air so the reflectivity signal comes only from the tethered PS block (the block of interest), and thus there is no need to subtract large corrections.

The second feature is that the degree of overlap of the PS blocks σ^* can be varied *continuously* either by varying the surface area for a fixed number of copolymer molecules in the monolayer, or by varying the number of copolymer molecules at fixed area. With adsorbed and grafted chains at the solid–liquid interface, σ^* for a particular system is fixed.[27] Variation of σ^* can only be achieved by varying the asymmetry of the copolymer[9-13,21,28] or the conditions of the grafting reaction.[15-17] With the present system, the upper limit of σ^* corresponds to the surface concentration at which the equilibrium spreading pressure is attained. For higher concentrations, the monolayer is unstable and copolymer molecules are lost into the bulk of the solution either as single chains or as micelles, depending on whether or not the critical micelle concentration has been reached in the bulk. There is no lower limit to the value of σ^* except the practical limit dictated by the fact that the magnitude of the reflectivity signal (difference from the Fresnel curve) will decrease as the surface concentration decreases.

We note that the range of attainable surface densities varies considerably among the various experimental systems. The highest values have been reported for terminally-grafted systems, where Auroy et al.[15-17] have reported values of σ^* greater than 70 and Cosgrove et al.[14] obtained values up to 11. In Auroy's work, the very high surface densities have apparently been achieved by performing the grafting reaction in the presence of a concentrated solution, where excluded volume repulsion effects are screened out. The systems were later swelled with a good solvent which introduces excluded volume interaction and causes the chains to stretch perpendicular to the surface. For the block copolymer adsorption work at the solid–liquid interface, maximum values range from 4 to 7.[20,21,28] The maximum value of σ^* obtained thus far in the present work is 4.2. Parsonage et al.[28] have shown that the maximum σ^* values for adsorbed block copolymer systems are obtained for copolymers which are highly asymmetric. Thus we expect that somewhat higher values of σ^* may be achieved in the present system with more highly asymmetric copolymers.

A third important feature is that the energy due to the interaction of the PS blocks is accessible through measurements of the surface pressure ($\Pi = \gamma_{EB} - \gamma$). Bringuier et al.[29] first showed that the electrostatic interaction between the dangling charged blocks in monolayers of PMMA–P4VP quaternized diblock copolymers on water produces a significant increase in the surface pressure over that of the homopolymer corresponding to the anchoring block. The increase in surface pressure ($\Delta\Pi$) was studied as a function of salt concentration in order to examine the effect of electrostatic screening. Granick and Herz[30] later showed that the osmotic interaction between the dangling PS blocks of a PDMS–PS diblock copolymer monolayer on the surface of tricresyl phosphate also produces a measurable increase. In both cases, the increase in surface pressure $\Delta\Pi$ can be related to the free energy of the dangling blocks F by $\Delta\Pi = -(\partial F/\partial \mathcal{A})_{n,T,P}$, where $\mathcal{A}$ is the surface area and n is the number of copolymer molecules, with the assumption that the anchoring block behaves in exactly the same manner upon compression as the homopolymer. *To our knowledge, this is the only direct measurement of the chain energy for a tethered chain system currently available.* By comparison, in the surface forces experiment the force required to compress the tethered layer perpendicular to the surface is obtained, while the free energy of an uncompressed layer is not accessible. Finally, chain energy has not been probed in the work involving chains end-grafted onto silica particles.

Thus with the present system, in principle, the concentration profile and the energy of the tethered blocks can be measured simultaneously as a continuous function of σ^*. A previous study[31] involving neutron reflectivity from polyacetylene–polyisoprene (2000–8000) diblock copolymers adsorbed from solution to the air-toluene interface has been reported, but it is the fact that the copolymer spreads to form a monolayer which is unique in this work and which allows the important variable σ^* to be varied continuously.

Experimental Section

The two PDMS–PS hydrogenated diblock copolymers which have been studied were generous gifts from Y. Gallot (ICS Strasbourg) and R. Jerome (Liege). They differ mainly in the molecular weight of the PDMS block, and their respective molecular weights and polydispersities are 10 500–40 000 (10–40) and 1.1, and 25 000–35 000 (25–35) and 1.2. PDMS homopolymer of 25 000 and $M_w/M_n = 3.9$ was kindly donated by Alain Lapp (LLB Saclay) and was used to assess the effect of the PS block through a comparison of the PDMS surface pressure isotherm with those of the block copolymers. The solvent was ethyl benzoate,[32] which is a nonsolvent for PDMS and a good solvent for PS.[33] The radius of gyration corresponding to free PS coils of molecular weight 40 000 and 35 000 are estimated to be 64 and 59 Å, respectively, from $R_g = 0.117 M_w^{0.595}$ for PS in toluene.[34] Surface tension measurements were performed with the Wilhelmy plate technique, using a sandblasted platinum plate 2 cm long and a Schenk force transducer. Typical reproducibility was ±0.2 dyne/cm. Selected measurements were also performed using a ring rather than a plate, to determine if adsorption onto the plate was important. We observed no difference in values measured by the two methods for either the homopolymer or block copolymer isotherms. The deuterated solvent was found to have the same surface tension (34.1 ± 0.3 dyne/cm) as that for the hydrogenated EB. In addition, equilibrium spreading pressures for the block copolymers were found to be the same (~9 dyne/cm) on the deuterated and hydrogenated EB. When spread from a chloroform solution, the PDMS homopolymer formed an insoluble monolayer on the surface of EB. On the contrary, when dry grains of PS homopolymer were deposited onto the surface of EB, the grains dissolved but no change in surface tension was observed. This indicates that PS does not spread to form a monolayer on EB but, equally importantly, also suggests that the dissolved PS does not adsorb at the surface.

Neutron reflectivity experiments were performed at the time-of-flight reflectometer DESIR in the ORPHEE reactor (Laboratory Leon Brillouin, Saclay). The sample was contained in an aluminum trough (95 × 30 × 2 mm), which was completely enclosed to minimize loss of solvent by evaporation. The neutron beam passed through quartz windows to enter and exit the sample cell chamber. The neutron wavelengths ranged from ~3 to 15 Å, and the incident angle and angular resolution were 0.97° and 5–10%, respectively. A range of momentum transfer vector q ($=4\pi(\sin\theta)/\lambda$) up to 0.045 Å^{-1} was used in the fits. Reflectivities were calculated from model profiles by approximating the exact profile with a series of thin homogeneous slabs and using the Fresnel coefficients to calculate the reflected and transmitted waves. Best fits were determined both by visual inspection and by minimization of χ^2 (good agreement was found between the two methods). Estimates of uncertainties in the fitting parameters correspond to roughly a 15% increase in χ^2 from the minimum values.

The measurement of the surface pressure isotherm for the PDMS homopolymer was performed with a Teflon trough and a sliding Teflon barrier. The polymer was spread from a chloroform solution, and the number of polymer molecules per area in the surface layer was determined from the concentration of the spreading solution and the volume deposited on the surface. However, since the density of chloroform is greater than that of EB, special precautions were required to ensure that drops of the spreading solvent did not pass into the bulk of the solution. The addition was performed by placing the drops on an inclined glass rod. The drops flowed down the rod and onto the surface of the solution. With this technique the measured isotherm was reproducible and independent of the number of drops initially added. However, we have been unable to use the same method to obtain the surface pressure isotherms for the block copolymers. The measured isotherms always varied with the number of drops of the spreading solution initially deposited, as well as with the concentration of the spreading solution. We conclude that some of the copolymer molecules are always lost into the bulk of the solution *during spreading* and, thus, that the number of copolymer molecules per unit area in the surface layer must be measured in situ. For this reason, we have determined the copolymer isotherms by estimating the surface concentration from the integral of profiles fit to the reflectivity data. We wish to emphasize that this difficulty is associated only with the spreading process and that once the monolayers are spread they are completely stable, i.e. the surface pressure does not vary with time (~15 h) and the isotherms are reproducible upon expansion and recompression.

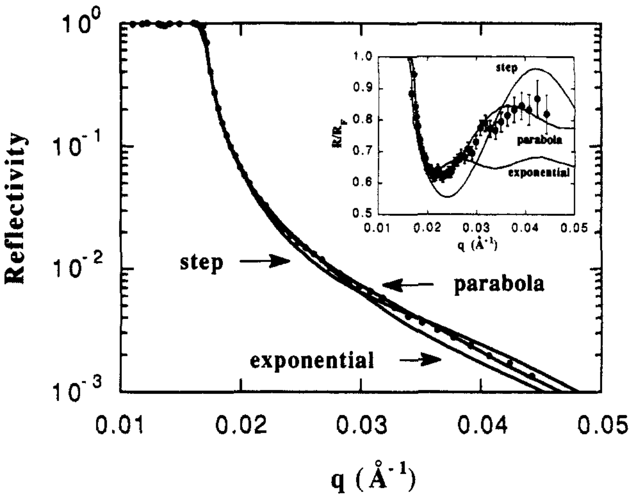

Figure 1. Comparison of calculated reflectivities using parabolic, exponential, and step profiles with experimental data for the 10–40 PDMS–PS diblock copolymer at $\sigma^* = 4.2$. The inset shows the reflectivity curves divided by the Fresnel curve for the pure solvent. The parabolic profile is consistent with the experimental data whereas the step and exponential profiles are clearly inadequate.

For the reflectivity measurements, the copolymer monolayers were spread by simply depositing a dry grain onto the surface of the EB subphase, in order to avoid the use of a spreading solvent and the uncertainty of whether some of the spreading solvent is retained in the surface layer. The surface tension was measured before and after each reflectivity measurement. The surface concentration was then either increased by further addition of grains to the surface or decreased by aspirating the surface. For a few measurements at low surface pressures, it was found that the surface pressure increased significantly on the time scale required for the reflectivity measurement (6–8 h). This was apparently due to excess polymer which had dissolved into the bulk of the solution when the dry grain was initially introduced and which slowly replenished the monolayer. When this occurred, the data acquisition was stopped after every hour and the surface aspirated until the initial surface pressure was obtained. The hourly spectra were added together to obtain a final spectrum with good statistics. In this way the variation in surface pressure was kept at an acceptably low level (<±1 dyne/cm). It was found that this problem could be largely eliminated by avoiding addition of an excess of copolymer to the surface. The reported surface pressures are averaged values.

Results and Discussion

The reflectivity curve for the highest value of σ^* (4.2) attained with the 10–40 copolymer is shown in Figure 1 along with best fits to parabolic, step, and exponential

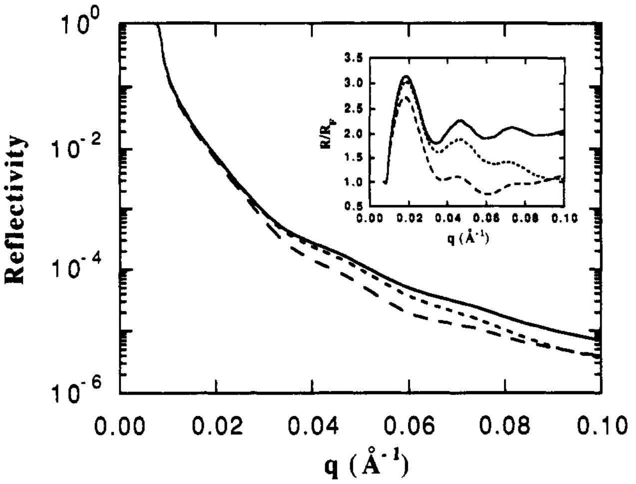

Figure 2. Simulated reflectivity curves for protonated EB and a PDMS–PS copolymer with the PS block deuterated. The solid curve corresponds to the parabolic profile obtained from a fit to the data in Figure 1 ($\phi_s = 0.128$, $h^* = 240$ Å). The dashed (short dashes) line corresponds to a profile with a 40-Å depletion layer defined as follows: The concentration is zero at the surface and then rises linearly with depth until $z = 40$ Å where it reaches the value of the parabolic profile. For $z > 40$ Å, the profile decays with the same parabolic profile as for the solid curve. The dashed (long dashes) line corresponds to a profile with a depletion layer of 80 Å defined in the same way. The inset shows the reflectivity divided by the Fresnel curve. The presence of a depletion layer is quite evident for $q > 0.05$ Å^{-1}.

profiles. The step and exponential profiles are clearly inadequate at this surface density as well as for all other surface densities measured, while the parabolic profile $\phi = A(h^{*2}-z^2)$ gives an adequate fit to the data up to $q = 0.04$ Å^{-1}. Here ϕ is the volume fraction polymer, z is the depth from the surface, h^* is the maximum extension from the surface, and the concentration at the surface is given by $\phi_s = Ah^{*2}$. The inset of Figure 1 shows the reflectivity divided by the Fresnel curve, which displays more clearly the structure in the reflectivity curve. The maximum extension h^* is found to be 240 ± 10 Å. The data for the present range of momentum transfer ($q < 0.05$ Å^{-1}) and reflectivity ($>10^{-3}$) are thus quite sensitive to the large-scale details of the profile. However, a q range extending to 0.06 Å^{-1} and reflectivity measured to 10^{-5} (which are well within the capabilities of current reflectometers, such as the CRISP reflectometer at the Rutherford Appleton Laboratory or the SPEAR reflectometer at Los Alamos) are required to examine finer details such as a small depletion layer near the surface or a tail in the profile near h^*. This is illustrated in Figure 2. This figure shows simulated reflectivity curves for a system with protonated EB and a PDMS–PS copolymer with a deuterated PS block, which gives greater contrast than the present system. Curves are shown for the parabolic profile determined from the data in Figure 1, as well as for profiles with depletion layers at the surface of 40 and 80 Å. These curves show that the reflectivity for the protonated EB/PDMS-*d*-PS system should be quite sensitive to the presence of a small depletion layer for $q > 0.05$ Å^{-1}. Thus while the parabolic profile is adequate to fit the present data over the present range of q, profiles similar in form or involving more parameters cannot be ruled out and we employ the parabolic profile for the present as a semiempirical fit involving the minimum number of adjustable parameters.

Next we discuss the variation in h* observed over the attainable range of σ^* (1.3–4.2). For $\sigma^* < 1$, one expects the rms dimension of the PS blocks to be constant with σ^* at a value roughly equal to the radius of gyration of a free coil in solution $R_{g,b}$. More precisely, MC simulations[35] have shown that for an isolated self-avoiding-walk coil attached at one end to an impenetrable, noninteracting wall, $R/R_b \cong 1.2$ (independent of molecular weight) where R and R_b are the end-to-end distances for the terminally attached chain and for the free coil in solution, respectively. As σ^* increases beyond unity, the theories described earlier predict that the PS blocks will stretch perpendicular to the surface as they begin to interact with one another. These predictions are modified somewhat if there is an attractive or repulsive interaction with the surface. In the present work, we believe from surface tension arguments that the air surface of EB is a slightly repulsive interface for PS, which should lead to a larger depletion layer at the surface than is predicted for a noninteracting surface. However, this effect may be reduced somewhat when the surface is nearly completely covered by the PDMS block. In that case, the adsorption or depletion of PS at the EB–PDMS interface will depend on the relative magnitudes of the interfacial energies $\gamma_{\mathrm{EB,PDMS}}$ and $\gamma_{\mathrm{PS,PDMS}}$. We plan to measure these interfacial energies in the future.

Table I
Results from Surface Tension and Reflectivity Measurements

$\Delta\Pi$[a] (dyne/cm)	σ^*[b] (σ/σ_0)	h^* (Å)	ϕ_s[c] (vol %)
	PDMS–PS 10–40		
0.2 ± 0.4	1.3	210 ± 20	4.5
0.3 ± 0.4	1.7	210 ● 15	6.0
1.0 ± 0.4	2.6	225 ● 15	8.5
1.0 ± 1.2	3.0	235 ● 15	9.3
2.1 ± 0.5	2.8	235 ± 15	8.8
2.6 ± 1.2	3.4	230 ± 15	11.0
2.7 ± 0.5	3.6	235 ± 10	11.3
3.0 ± 0.5	4.1	235 ± 10	12.8
5.0 ± 0.4	4.0	240 ± 10	12.3
5.6 ± 0.8	4.2	240 ± 10	12.8
7.4 ± 0.8	4.2	240 ± 10	12.8
	PDMS–PS 25–35		
0.9 ± 0.3	2.2	200 ± 10	8.3
1.1 ± 0.5	2.6	215 ± 10	9.3
1.6 ± 0.5	3.0	230 ± 10	10.0
2.2 ± 0.3	3.0	225 ± 10	10.3

[a] The uncertainties include the variation of the surface pressure during the reflectivity measurement as well as the reproducibility of a single surface tension measurement. [b] The density of PS in the melt state (1.05 g/cm^3) was used in the calculation of the surface densities. [c] ±0.5 vol %.

Table I gives the surface pressure excess $\Delta\Pi$, the reduced surface density σ^*, and the parameters ϕ_s and h^* determined from fits of the reflectivity data to a parabolic profile for the two copolymers studied. We find that as the reduced surface density σ^* is increased from 1.3 to 4.2, there is a large increase in ϕ_s from 4.5% to 12.8%, but only a small (~15%) variation from 210 to 240 Å is observed in h^*. Figure 3 shows h^* for the 10–40 copolymer plotted versus σ^*. The value of h^* (240 Å) at the highest density is larger than the estimated radius of gyration (64 Å) and the distance between anchoring points (55 Å) by factors of 3.7 and 4.4, respectively. We estimate the degree of stretching perpendicular to the surface as the ratio of the average (rms) distance from the surface for the parabolic profile ($h_{\mathrm{rms}} = h^*/5^{1/2} = 107$ Å) to the rms radius of gyration (64 Å), which gives a value of 1.7. Thus it appears as if the PS block is stretched somewhat perpendicular to the surface at $\sigma^* = 4.2$. At the lowest surface density ($\sigma^* = 1.3$), the PS blocks still seem to be stretched slightly, as we observe a ratio of 1.5 rather than 1.2, as expected from MC simulations for isolated chains. Unfortunately, the low reflectivity signal for the present system at smaller σ^*

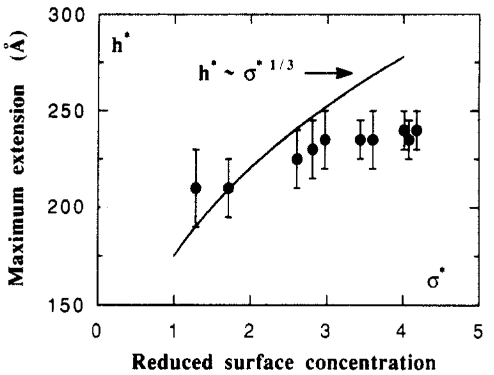

Figure 3. Variation of the maximum extension h^* (determined from fits of a parabolic profile to reflectivity data) with the reduced surface density σ^* (determined from the integral of the parabolic profiles) for the 10–40 PDMS–PS diblock copolymer. The variation is much weaker than $h^* \sim \sigma^{*1/3}$ predicted for the strongly stretched regime. The error bars correspond to uncertainty from the fitting (see Table I).

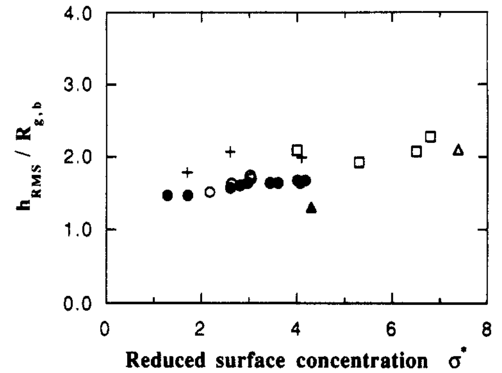

Figure 4. Variation of the average dimension of the concentration profile scaled by the radius of gyration with reduced surface density σ^* for data reported in the literature for PS in good solvents. The parameter $h_{\mathrm{rms}} = h^*/5^{1/2}$ is the rms average dimension of a parabolic concentration profile, while $R_{\mathrm{g,b}}$ is the estimated rms radius of gyration for a free coil corresponding to the tethered block in dilute solution. The data were taken from the following sources: (filled and open circles) present data 10–40 and 25–35, respectively; (filled triangle) ref 20; (open squares) ref 21; (crosses) ref 10; (open triangle) ref 12.[36]

does not allow the determination of the dimension of noninteracting submerged PS blocks ($\sigma^* < 1$). However, calculations indicate that the measurable range of σ^* should extend to much lower values with protonated EB and copolymers with deuterated PS blocks, and such experiments are currently underway.

The observed variation in h^* is not in agreement with the $^1/_3$ power law dependence predicted for the strongly stretched regime, represented by the solid line in Figure 3. This may suggest that this regime in only attained at higher values of σ^*. It is possible that the transition from the regime of isolated, noninteracting PS blocks to the strongly interacting regime does not occur abruptly at $\sigma^* = 1$, but may occur gradually, only reaching the strongly interacting regime when $\sigma^* \gg 1$. However, we note that we have observed no trend toward an increasing dependence of h^* on σ^* over the current range of σ^*. It is also possible that there are deviations from a parabolic profile at low σ^* (such as the presence of a depletion layer) which are unobservable in the present data due to low signal at the lowest σ^* and the limited q range. The presence of a depletion layer would lead to some ambiguity in the determination of h^*. We have determined that the maximum size of the depletion layer (distance between the surface and the maximum in the profile) which could be present, i.e. for which the reflectivity data could no longer be well fit by a parabolic profile over the present q range, is ~40 Å for the data at the highest surface density and ~80 Å for the data at the lowest surface density. This corresponds to an uncertainty in the surface density of roughly 13% and 30%, respectively. More importantly, this may explain why $h_{\mathrm{rms}}/R_{\mathrm{g,b}}$ appears to remain greater than 1.2 even at $\sigma^* = 1.3$.

The dimension h^* may be compared with that measured by other techniques for tethered PS chains in good solvents. To compare with data involving a range of molecular weights, we compare the scaled dimension $h_{\mathrm{rms}}/R_{\mathrm{g,b}}$ (Figure 4) over the reported ranges of σ^*. We have attempted to include all relevant data for which estimates of the surface concentration are available.[36] The type of scaling used in Figure 4 is actually only expected to hold for noninteracting tethered chains ($\sigma^* \lesssim 1$), where $h_{\mathrm{rms}}/R_{\mathrm{g,b}}$ should be roughly 1.2, independent of σ^*. Surprisingly, the data from many different laboratories involving several experimental techniques seem to conform to this scaling rather well even for σ^* up to 8. We observe that the present data are in general agreement with the maximum dimensions measured by other techniques. Figure 5 shows a log–log plot of the same data scaled as $h^*/N \sim \sigma$. The solid line indicates the predicted $^1/_3$ power law dependence. While the logarithmic scale masks somewhat the scatter in the data, it appears that all the data taken together do not conform well to this type of scaling over the range of surface densities corresponding to σ^* from 1 to 8. This is a tentative conclusion which awaits a larger body of data for confirmation.

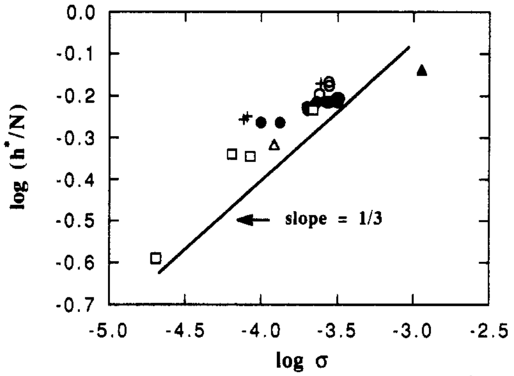

Figure 5. Variation of the average dimension of the concentration profile scaled by the molecular weight with surface density σ for data reported in the literature for PS in good solvents. The symbols have the same meaning as in Figure 4. The solid line indicates the predicted $^1/_3$ power law dependence.

In Figures 4 and 5 we have not included the data of Auroy et al.[15-17] involving end-grafted PDMS chains in the good solvent dichloromethane since the comparison of data from different chemical systems on an absolute scale requires precise values of the statistical segment lengths and excluded volume parameters. In addition, their data cover a much larger range of σ^*. They have reported $L_{\mathrm{rms}}/R_{\mathrm{g,b}}$ of ~1, virtually independent of σ^* up to $\sigma^* \cong 10$ (where L is the dimension of a step concentration profile fit to their data),[37] which is somewhat at odds with the data in Figure 4 which show some increase with σ^* over this range. For $\sigma^* > 10$, they observe a sharp rise in $L_{\mathrm{rms}}/R_{\mathrm{g,b}}$ to values greater than 3[17] and good agreement with $L \propto N\sigma^{1/3}$.[15] Thus, their results would suggest that the strongly stretched regime is only achieved for very large σ^*, which has so far been unattainable with the other systems. Clearly, more experiments on a variety of systems are required to definitively characterize the transition from the nonstretched regime to the strongly stretched regime.

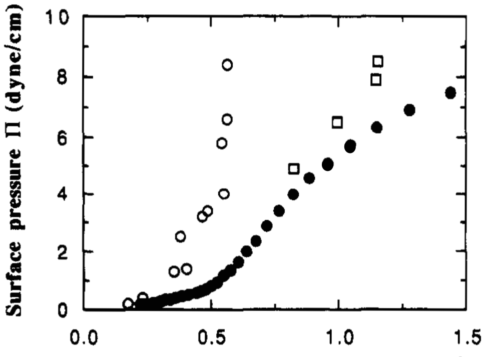

Figure 6. Surface pressure Π versus surface concentration of the anchoring block (PDMS) for the PDMS homopolymer (filled circles) and PDMS–PS diblock copolymers 10–40 (open circles) and 25–35 (open squares). The free energy of the submerged PS blocks is related to the increase in surface pressure for the block copolymers relative to the homopolymer (ΔΠ).

Next we discuss the variation in the free energy arising from the interaction of the PS blocks F_{PS} with σ^*, where F_{PS} is related to the surface pressure excess by $\Delta\Pi = -(\partial F_{PS}/\partial \mathcal{A})_{n,T,P}$. The isotherms are shown in Figure 6, where the ordinate is the surface concentration of PDMS. The rationale for representing the surface concentration in this way is that, since the isotherms for the PDMS homopolymer are independent of molecular weight (as observed for PDMS monolayers on tricresyl phosphate[30] and on water[38,39]), any increase in surface pressure for the block copolymer over that of the PDMS homopolymer at the same PDMS surface concentration must be due to the PS blocks. Thus, in principle, the free energy contributed by the PS blocks may be obtained from the difference ΔΠ of the surface pressures of the copolymer and the homopolymer monolayers for a given PDMS surface concentration, assuming that the PDMS block of the block copolymer behaves in exactly the same way with changes in σ as the PDMS homopolymer.

We find that the PDMS monolayer is of the expanded type, with the gradual increase in surface pressure with surface concentration at low surface concentrations representing the compression of a two-dimensional gas of molecules on the surface. The more rapid rise beginning near 0.6 mg/m² represents the completion of a full monolayer. The leveling off of the surface pressure at higher surface concentrations is believed to be due to some sort of collapse of the monolayer. This isotherm is similar to that observed for PDMS on tricresyl phosphate[30] but is in contrast to that observed on water,[38,39] where little or no pressure is observed until monolayer coverage is approached (~0.7 mg/m²). The lack of surface pressure at low surface coverages on water is believed to be due to the formation of aggregates of PDMS molecules, or islands, on the surface. At full monolayer coverage, the thickness of a PDMS monolayer on water has been determined from neutron reflectivity to be roughly 8 Å.[40]

To determine whether there may be some aggregation of the PDMS molecules on EB, we have compared the surface pressure data at low surface concentrations with the ideal gas law. For low surface concentrations, one can express the surface pressure as a virial expansion:

$$\Pi = RT(\Gamma + A_{22}{}^{\Gamma}\Gamma^2 + ...) \qquad (1)$$

where Γ is the surface concentration in moles per square centimeter (where the number average molecular weight is used to calculate Γ for polydisperse samples) and $A_{22}{}^{\Gamma}$ is the surface second virial coefficient. Therefore, a plot of $\Pi/\Gamma RT$ versus Γ for low Γ should be linear with a slope equal to $A_{22}{}^{\Gamma}$ and an intercept of 1. If there is some aggregation of the molecules forming the monolayer, a lower intercept is observed. Figure 7 shows the surface pressure data for PDMS on EB plotted according to eq 1. The solid line is a least-squares fit through the first eight data points. The slope indicates a positive second virial coefficient (~4.2 × 10¹¹ ± 0.2 × 10¹¹ cm²/mol), with an intercept of 0.60 ± 0.40. Unfortunately, the precision of the current measurement technique precludes the acquisition of data at lower surface concentrations from which the extrapolation to zero concentration could be made with less uncertainty. However, the present data seem to exclude the possibility of large aggregates which would have resulted in an extrapolated value of $\Pi/\Gamma RT$ near zero. If the concentration range used for the extrapolation in Figure 7 is high enough that a small contribution from the Γ^3 term is present, then the true intercept which would be obtained from data extrapolated over a lower concentration range will be higher. This likely explains the difference between the measured value of 0.6 and unity.

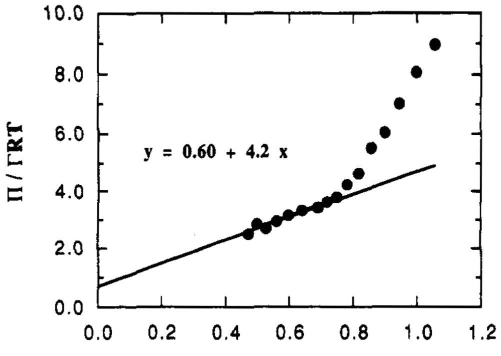

Figure 7. Surface pressure of PDMS on EB for low surface concentrations plotted according to eq 1. The solid line is a least-squares fit to the data for the lowest eight surface concentrations. The presence of large aggregates on the surface would have led to an intercept close to zero.

In Figure 6, we find that the isotherms rise more rapidly for the copolymers than for the homopolymer, presumably due to the interaction of the PS blocks, and that the deviation from the isotherm of the homopolymer occurs at higher values of the ordinate for the 25–35 copolymer than for the 10–40 copolymer. Apparently, this is because higher PDMS surface concentrations are required to achieve the same degree of crowding of the PS blocks (the same σ^*) for the copolymer with the larger PDMS block. This is shown more clearly in Figure 8, in which ΔΠ is plotted versus σ^* for the two copolymers. The fact that the data fall onto the same curve in this representation is strong evidence that the surface pressure excess ΔΠ is due to the interaction of the PS blocks.

The isotherms for the block copolymers in Figure 6 are somewhat different than those reported by Granick et al.[30] for monolayers of PDMS–PS diblock copolymers on tricresyl phosphate (the system is similar to that in the present work in that the PDMS block remains on the surface while the PS block is soluble in the subphase). In the present work, the deviation from the isotherm of the homopolymer occurs at lower surface concentrations of the anchoring PDMS block (for the 10–40 copolymer which may be compared to their data for a 14–44 copolymer), and the copolymer isotherms in Figure 6 rise more steeply than those of Granick et al. We believe these differences are due to the different methods of measuring the surface concentration, which is important because of the problem discussed in the Experimental Section that copolymer

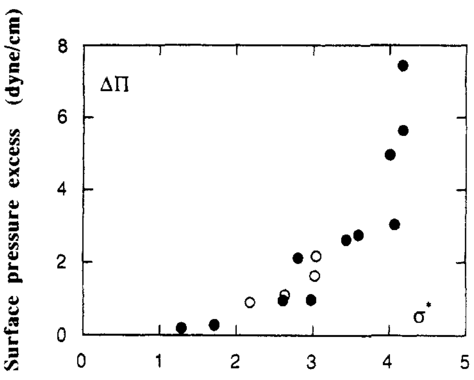

Figure 8. Variation of the surface pressure excess (ΔΠ) with reduced surface density σ^*. The fact that the data appear to collapse to the same curve in this representation (for copolymers in which the molecular weight of the PDMS block varies by a factor of 2.5) is evidence that ΔΠ is due to the interaction of the PS blocks.

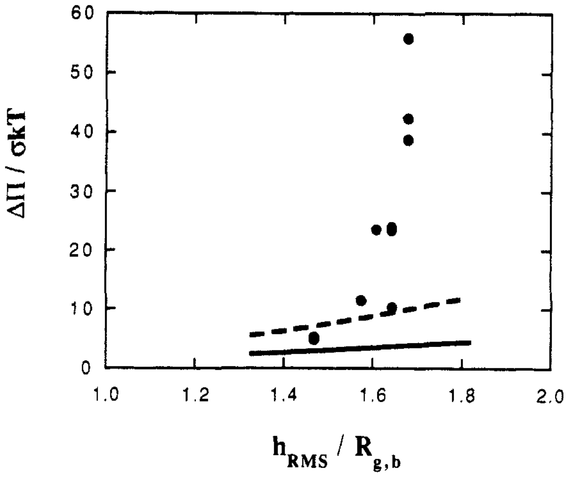

Figure 9. Variation of $\Delta\Pi/\sigma kT$ with reduced extension $h_{\mathrm{rms}}/R_{\mathrm{g,b}}$ for the 10–40 PDMS–PS copolymer. The solid line is the self-consistent mean-field prediction from ref 41, with the monomer length chosen as 7.6 Å. The dashed line shows the dependence predicted for a swollen polymer brush from ref 3. These data suggest that there is a much larger energetic barrier for chain stretching in this system than is predicted by current theories.

molecules may be lost into the bulk of the solution during spreading. In their work, the surface concentrations were calculated from the concentration of the spreading solution and the volume of solution deposited onto the surface, assuming no loss of copolymers into the bulk, whereas in the present work the surface concentrations are measured in situ by neutron reflectivity. We noted above that the isotherms for the present system determined by the former method were not reproducible and varied greatly with the volume of spreading solution initially deposited onto the surface. From this we conclude that there is always some loss of copolymer molecules into the bulk during spreading and that the surface concentration must be measured in situ.

In Figure 9 $\Delta\Pi/\sigma kT$ for the 10–40 copolymer is plotted against $h_{\mathrm{rms}}/R_{\mathrm{g,b}}$ for the range of attainable σ^*. We find that the ordinate is an extremely rapidly increasing function of h_{rms} for $h_{\mathrm{rms}}/R_{\mathrm{g}} > 1.6$. The analytic self-consistent field theory of Milner, Witten, and Cates[3,41] predicts

$$f = (9/10)(\pi^2/12)^{1/3} N \sigma^{5/3} w^{2/3} \nu^{1/3} \qquad (2)$$

$$h^* = (12/\pi^2)^{1/3} N \sigma^{1/3} w^{1/3} \nu^{-1/3} \qquad (3)$$

where f is the free energy per unit area of the polymer brush in units of kT, N is the number of PS monomers per block, w is the excluded volume parameter, and ν is related to the monomer length a by $3/\nu = a$. Since $F_{\mathrm{PS}}/kT = \mathcal{A}f$ and $\sigma = n/\mathcal{A}$, these equations lead to $\Delta\Pi/kT = (2/3)f$ and

$$\Delta\Pi/\sigma kT = (2/3)(9/10)(\pi^2/12)(h^{*2}/N)(3/a^2) \qquad (4)$$

This relation is represented by the solid line in Figure 9. The only adjustable parameter is the monomer length, which we have chosen as 7.6 Å as in ref 41. The experimental data indicate a much steeper dependence on h^*, and thus a much larger energetic barrier for chain stretching, than is predicted by this theory. (The prediction of the Alexander theory differs from that of MWC by only a numerical factor of order unity.) The lack of agreement shown in Figure 9 is especially surprising since this theory has been reported to be in quantitative agreement with results from the force-balance apparatus for layers of end-anchored PS chains of molecular weight 141 000,[41] where the two layers of tethered chains are compressed perpendicular to the surfaces (the present data correspond to a compression of the tethered layer parallel to the surface). We note that the self-consistent field analysis is only strictly valid for high monomer concentrations and/or small excluded volume parameter and that the relatively low monomer concentrations of the layers in the present work (<13%) may warrant comparison with the swollen brush predictions, where $\Delta\Pi/\sigma \sim h^{*2.5}$. This dependence is shown by the dotted line in Figure 9. The improvement is very slight, and the agreement is still poor.

The origin of the sharp increase in surface pressure with surface concentration and the lack of a corresponding increase in h^* are unexplainable at present. We note that Ligoure[42] has proposed the formation of surface micelles under certain conditions when the anchoring block does not completely wet the surface. The surface tension for the PDMS/EB interface is not known at present, so the spreading coefficient $S = \gamma_{\mathrm{AIR/EB}} - \gamma_{\mathrm{AIR/PDMS}} - \gamma_{\mathrm{EB/PDMS}}$ cannot yet be calculated. Since $\gamma_{\mathrm{AIR/EB}} \cong 34.1$ dyne/cm and $\gamma_{\mathrm{AIR/PDMS}} \cong 20$, partial wetting will be expected if $\gamma_{\mathrm{EB/PDMS}} > 14$ dyne/cm. In that case the formation of surface micelles remains a possibility. However, the surface pressure data for PDMS at low surface concentrations seems to exclude the possibility of large aggregates. In addition, the fact that ΔΠ for the two block copolymers collapsed to a single curve when plotted versus σ^* also argues against the formation of surface micelles, as the structure of the surface micelles is expected to be highly dependent on the asymmetry of the copolymer. The presence of glassy PS near the surface could also conceivably lead to large ΔΠ (a thin ~10-Å melt layer of PS would be unobservable in the reflectivity experiment over the present q range). However, as EB is known to be a good solvent for PS and surface tension measurements suggest the presence of a depletion layer rather than adsorption of PS at the surface, this seems unlikely. It is hoped that further insight can be gained from further measurements with deuterated PS blocks at higher q and by varying the molecular weight of the PS block and the quality of the solvent.

In summary, we report experimental measurements of both the concentration profile and the free energy of a tethered chain system as a function of the distance between anchoring points. A parabolic profile is found to give the best fit to the reflectivity curves among the set of two-parameter models examined. The extension $h_{\mathrm{rms}}/R_{\mathrm{g,b}}$ agrees well with values measured by other techniques for similar σ^*; however, the dependence on σ^* is much weaker than the $^1/_3$ power law predicted for the strongly stretched regime. An important observation from this work is that for the highest values of σ^* we observe a sharp rise in $\Delta\Pi$ with little or no change in the maximum extension h^*. This may indicate that the free energy required for chain stretching in this system is much larger than predicted by current theories. For the future, calculations have shown that the use of polymers with deuterated PS blocks will greatly increase the reflectivity signal, allowing a more detailed characterization of the concentration profile and the range of σ^* to be extended to lower values. We hope to achieve higher σ^* values by using more highly asymmetric polymers. In addition, we plan to measure the dependence of h^* on the molecular weight of the PS block over the range of assessible σ^* and to vary the quality of the solvent for the PS block.

Acknowledgment. This work has been partially supported by the Societé Nationale Elf Aquitaine (Departement de la Recherche, du Developement et de l'Innovation). M.K. has been the recipient of a postdoctoral fellowship from Elf Aquitaine and a grant from the CNRS.

References and Notes

(1) For a review, see: Halperin, A.; Tirrell, M.; Lodge, T. P. *Adv. Polym. Sci.* **1992**, *100*, 31.
(2) Alexander, S. *J. Phys. (Paris)* **1977**, *38*, 977.
(3) Milner, S. T.; Witten, T. A.; Cates, M. E. *Europhys. Lett.* **1988**, *5*, 413; *Macromolecules* **1988**, *21*, 2610.
(4) Zhulina, E. B.; Borisov, O. V.; Pryamitsin, V. A. *J. Colloid Interface Sci.* **1990**, *137*, 495.
(5) Dolan, A. K.; Edwards, S. F. *Proc. R. Soc. London* **1975**, *A343*, 427.
(6) Hirz, S. J., M.S. Thesis, University of Minnesota, 1986.
(7) Cosgrove, T.; Heath, T.; van Lent, B.; Leermakers, F.; Scheutjens, J. H. M. S. *Macromolecules* **1987**, *20*, 1692.
(8) Muthukumar, M.; Ho, J. S. *Macromolecules* **1989**, *22*, 965.
(9) Hadziioannou, G.; Patel, S.; Granick, S.; Tirrell, M. *J. Am. Chem. Soc.* **1986**, *108*, 2869.
(10) Patel, S.; Hadziioannou, G.; Tirrell, M. *Proc. Natl. Acad. Sci. U.S.A.* **1987**, *84*, 4725.
(11) Patel, S.; Tirrell, M. *Annu. Rev. Phys. Chem.* **1989**, *40*, 597.
(12) Taunton, H. J.; Toprakcioglu, C.; Fetters, L. J.; Klein, J. *Nature* **1988**, *332*, 712; *Macromolecules* **1990**, *23*, 571.
(13) Taunton, H. J.; Toprakcioglu, C.; Klein, J. *Macromolecules* **1988**, *21*, 3333.
(14) Cosgrove, T. *J. Chem. Soc., Faraday Trans.* **1990**, *86*, 1323.
(15) Auroy, P.; Auvray, L.; Léger, L. *Phys. Rev. Lett.* **1991**, *66*, 719.
(16) Auroy, P.; Auvray, L.; Léger, L. *Macromolecules* **1991**, *24*, 2523.
(17) Auroy, P.; Auvray, L.; Léger, L. *Macromolecules* **1991**, *24*, 5158.
(18) Blum, F. D.; Sinha, B. R.; Schwab, F. C. *Macromolecules* **1990**, *23*, 3592.
(19) Satija, S. K.; Majkrzak, C. F.; Russell, T. P.; Sinha, S. K.; Sirota, E. B.; Hughes, G. J. *Macromolecules* **1990**, *23*, 3860.
(20) Cosgrove, T.; Heath, T. G.; Phipps, J. S.; Richardson, R. M. *Macromolecules* **1991**, *24*, 94.
(21) Field, J. B.; Toprakcioglu, C.; Ball, R. C.; Stanley, H. B.; Dai, L.; Barford, W.; Penfold, J.; Smith, G.; Hamilton, W. *Macromolecules* **1992**, *25*, 434.
(22) Chakrabarti, A.; Toral, R. *Macromolecules* **1990**, *23*, 2016.
(23) Murat, M.; Grest, G. S. *Phys. Rev. Lett.* **1989**, *63*, 1074; *Macromolecules* **1989**, *22*, 4054; *Macromolecules* **1991**, *24*, 704.
(24) Kent, M. S.; Lee, L. T.; Rondelez, F. Submitted for publication to *Europhys. Lett.*
(25) The value for PDMS was taken from *Silicone Compounds*, Petrarch Systems Silanes and Silicones, the value for EB was measured in this work, and the value for PS was taken from: Brandrup, J.; Immergut, E. H. *Polymer Handbook*, 3rd ed.; John Wiley & Sons: New York, 1989.
(26) Guiselin, O.; Lee, L. T.; Farnoux, B.; Lapp, A. *J. Chem. Phys.* **1991**, *95* (6), 4632.
(27) In the former case this is due to the near irreversibility of the adsorption for strongly adsorbing systems.
(28) Parsonage, E. E.; Tirrell, M.; Watanabe, H.; Nuzzo, R. G. *Macromolecules* **1991**, *24*, 1987.
(29) Bringuier, E.; Vilanove, R.; Gallot, Y.; Selb, J.; Rondelez, F. *J. Colloid Interface Sci.* **1985**, *104*, 95.
(30) Granick, S.; Herz, J. *Macromolecules* **1985**, *18*, 460.
(31) Dai, L.; White, J. W.; Kerr, J.; Thomas, R. K.; Penfold, J.; Aldissi, M. *Synth. Met.* **1989**, *D69–D89*, 28.
(32) Fully deuterated EB was specially synthesized for this work by J. P. Roque (USTL), Montpellier), and protonated EB was purchased from Aldrich. Both were distilled under vacuum just prior to use.
(33) Previous measurements (higher M_w) have shown that R_g for PS is nearly the same in EB as in toluene. Kent, M. S.; Tirrell, M.; Lodge, T. *Polymer* **1991**, *32* (2), 314.
(34) Higo, Y.; Ueno, N.; Noda, I. *Polym. J.* **1983**, *15*, 367.
(35) Hahn, T. D.; Kovac, J. *Macromolecules* **1990**, *23*, 5153.
(36) There is some subjectivity in choosing the maximum extension in the force balance experiment. Our estimates for twice the maximum extension from the data in ref 10 are 650 (60–60), 960 (60–90), and 650 (5–50). We have not included the data for the 60–150 copolymer in ref 10 because the long tail unique to this set of data makes an estimate of the maximum dimension highly uncertain. Our estimates for σ^* for these data come from the correlation in ref 28.
(37) To estimate $R_{g,b}$ for the data of refs 15–17, we have used $R_g = 0.124M^{0.605}$ for PDMS in toluene taken from the data in ref 26.
(38) Granick, S. *Macromolecules* **1985**, *18*, 1597.
(39) Mann, E. K.; Langevin, D. *Langmuir* **1991**, *7*, 1112.
(40) Lee, L. T.; Mann, E. K.; Langevin, D.; Farnoux, B. *Langmuir* **1991**, *7*, 3076.
(41) Milner, S. *Europhys. Lett.* **1988**, *7* (8), 695.
(42) Ligoure, C. *Macromolecules* **1991**, *24*, 2968.